JOURNAL OF MATERIALS SCIENCE 20 (1985) 1079–1084

Characterization of Fe(III)–Zr(IV) mixed and Sn(III)-doped hydrous oxides

S. K. SRIVASTAVA, C. K. JAIN
Department of Chemistry, University of Roorkee, Roorkee-247667, India

Surface and structural properties of iron–zirconium mixed and Sn(II)-doped hydrous oxide gels have been compared with ferric oxide hydrate gel using thermal analysis, infrared spectroscopy, X-ray diffraction, electron microscopy and magnetic measurements. The mixed and doped oxide gels were found to consist of a hexagonal close packed arrangement of oxygen sublattices similar to those present in α-FeOOH and α-Fe_2O_3, with the iron ion quite randomly distributed in the gels. The gels were found to be composed of hexagonal to rounded and thin rod-like particles and their agglomerates. The particles in the superparamagnetic state have an incompletely compensated antiferromagnetic character.

1. Introduction

Iron oxides find wide applications as catalysts, adsorbants, pigments, surface coatings and also as advance technology materials used in the production of bubble ferrites and magnetic tapes [1, 2]. Recently Dutta [3] has discussed and reviewed the detailed aqueous and solid state chemistry of well characterized crystalline iron oxides and oxyhydroxides. Zirconium oxide gels are also interesting substances, which have found use as starting materials for the production of high-area ZrO_2, for its use as refractory or support material [4, 5]. It is certain that the application of these materials is markedly dependent upon the method of preparation and there are a number of papers [6–8] in which different aspects of these systems have been analysed.

It is worth pointing that the investigations in this direction are limited to pure hydrous oxides and no effort has been made to correlate the surface and structural properties of mixed oxide

In this paper we attempt to characterize structurally the iron–zirconium mixed oxide compared to the pure oxide and we have also observed the effect of doping with Sn(II) cation.

2. Experimental techniques

2.1. Materials

Ferric chloride (BDH), zirconium oxychloride (AR) and stannous chloride (AR) were used as such and their solutions were prepared in double distilled water.

2.2. Preparation of mixed and doped hydrous oxide gels

Ferric chloride (0.2 M) and zirconium oxychloride (0.2 M) were mixed to give a molar ratio of 8 : 1 (optimum conditions at which the product shows maximum anion as well as cation exchange capacity). The mixed hydrous oxide was coprecipitated slowly under constant sitrring. The precipitate was left to stand with the mother liquor for 2 days at room temperature, washed several times by decantation with distilled water, filtered and dried at 80° C for 24 h. Doped oxide was prepared by adding 0.075 g $SnCl_2$ to a 450 ml solution of ferric chloride and zirconium oxychloride in a molar ratio of 8 : 1, and was also precipitated with ammonium hydroxide.

2.3. Techniques used

Thermal analysis, infrared spectroscopy, X-ray diffraction, electron microscopy and magnetic measurements are the techniques used to characterize the gels.

Differential thermal curves were recorded on a Fisher Differential Thermalyser model 260 P and thermogravimetric curves on a Stanton Redcroft

0022–2461/85 $03.00 + .12

TG-770 model instrument. Samples were passed through 100 mesh size sieves and heated in air in a platinum crucible from room temperature to 1000° C at a rate of 10° C min^{-1}.

Infrared spectra were recorded with a Beckmann model IR-20 spectrophotometer operated in the double beam mode. The samples were used in the form of KBr pellets.

Diffraction patterns were recorded at room temperature at a speed of 2θ deg min^{-1} (ranging from 1 to 2° min^{-1}) in Phillips Type PW 1140/9P X-ray diffractometer using zirconium-Mo$K\alpha$ radiation = 0.0711 nm.

Transmission electron micrographs were recorded with a Phillips EM-400 transmission electron microscope at 80 to 100 kV. Samples were prepared by dilution of a small quantity in absolute alcohol after dispersing the sample in an ultrasonic bath. Droplets of the diluted sample were taken from the middle of the test tube and placed on 200 mesh copper grids covered with a thin film of formvar. All the grids had been examined in the electron microscope prior to sample deposition.

Magnetic susceptibility measurements were performed using a Vibrating Sample Magnetometer model 155. Samples (0.05 to 0.10 g) were taken in the form of cylindrical pellets. The system was calibrated using the 3/32 in. x 3/32 in. cyclindrical sample of high-purity nickel. The saturation moment of the nickel sample was found to be about 55 emu g^{-1} with a saturation flux of about 8000 G.

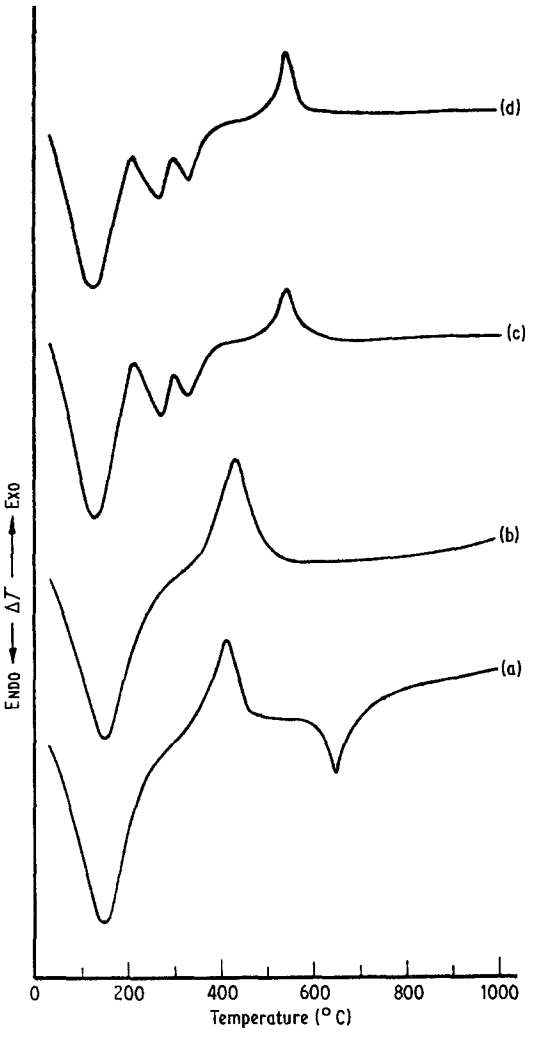

Figure 1 DTA curves of hydrate gels: (a) ferric oxide; (b) zirconium oxide; (c) Fe–Zr mixed oxide; (d) Sn(II)-doped oxide.

3. Results and discussion

3.1. Thermal analysis

Differential thermal and thermogravimetric curves for ferric oxide, zirconium oxide, Fe–Zr mixed oxide and Sn(II)-doped oxide hydrate gels are shown in Figs. 1 and 2, respectively.

The DTA curve of the ferric oxide hydrate gel (Fig. 1a) exhibits a sharp endothermic peak centred around 150° C and a strong exothermic peak at 410° C. These features correspond to the dehydration and dehydroxylation of the gel and crystallization of haematite. Furthermore, the distinct endothermic effect with a peak at 650° C marks the occurrence of a magnetic phase change – Neel transition [6, 9]. However, the value of the Neel point observed in the present study is lower in comparison to the normally reported value of 685° C [6, 9]. The DTA curve of zirconium oxide hydrate gel (Fig. 1b) shows an initial endothermic peak at 150° C, corresponding to dehydration, followed by a strong sharp exothermic peak at 430° C (the so-called glow phenomenon) due to the transition of ZrO_2 from an amorphous to a crystalline state [8, 10].

The DTA curves of Fe–Zr mixed and Sn(II)-doped oxide hydrate gels (Figs. 1c and d) show endothermic effects with peaks at 130, 270 and 330° C, corresponding to the removal of adsorbed water molecules and the removal of structural hydroxyl groups along with the desorption of ammonia and/or carbon dioxide. The splitting of the endothermic effect of dehydration into distinct peaks (Figs. 1c and d) possibly points to the structural inhomogeneity of the samples, suggesting

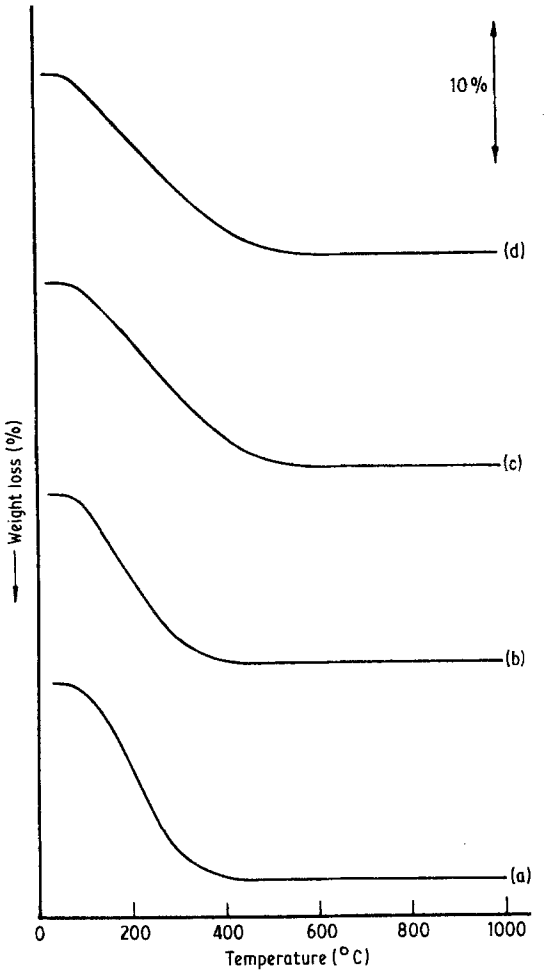

Figure 2 TGA curves of hydrate gels: (a) ferric oxide; (b) zirconium oxide; (c) Fe–Zr mixed oxide; (d) Sn(II)-doped oxide.

that more than one type of phase possessing distinct features is simultaneously present in the gel. The exothermic effect around 540° C corresponds to the simultaneous occurrence of disproportionating reactions involving removal of structural inhomogeneities associated with the appearance of nonstoichiometric phases and the crystallization of mixed oxides. Another distinguishing feature of mixed oxide hydrate gels is that the water is more firmly held in the gels, as compared to that in ferric oxide or zirconium oxide hydrate gels.

The TG results (Fig. 2) show that the loss in weight takes place in different steps in a continuous manner at temperatures corresponding to the endothermic and exothermic peaks in the DTA curves. The TG curves show a total weight loss of 14.0% for ferric oxide, 12.0% for zirconium oxide, 13.2% for Fe–Zr mixed and 13.1% for Sn(II)-doped oxide hydrate gels, respectively.

3.2. Infrared spectroscopy

The infrared spectra of ferric oxide hydrate gel show broad absorption bands centred at 3440 and 1640 cm^{-1} due to characteristic stretching and bending modes of vibrations for water and structural hydroxyl groups [11, 12]. Furthermore, the broad absorption bands in the 300 to 700 cm^{-1} region are due to iron–oxygen lattice vibrations.

According to Kauffman and Hazel [13], the region from 600 to 1100 cm^{-1} corresponds to bending vibrations of different ferric oxyhydroxides. The peaks correspond to O–H . . . O bending vibrations at 900 and 800 cm^{-1} for α-FeOOH, while those at 1020 and 745 cm^{-1} are for γ-FeOOH, and a weak and variable peak at about 840 cm^{-1} for β-FeOOH.

The infrared spectrum of the gel shows peaks at 790 and 890 cm^{-1} corresponding to the OH . . . O bending frequencies of α-FeOOH. A single strong broad band centred around 580 cm^{-1} observed for this gel indicates a hexagonal close packed arrangement of oxygen sub-lattices similar to those present in α-FeOOH and α-Fe_2O_3 with iron ions being quite randomly distributed in the gel. Thus the features observed here support the formation of α-Fe_2O_3 and α-FeOOH phases in the gel under study.

The infrared spectra of Fe–Zr mixed and Sn(II)-doped oxide hydrate gels compare well with the infrared characteristics of ferric oxide hydrate gel. For α-Fe_2O_3, the infrared spectra display a very broad band in the low-frequency region with absorption centred around 400 and 580 cm^{-1}, while for α-FeOOH it lies at 800 and 900 cm^{-1}. The infrared spectrum of hydrous zirconium oxide gel is characterized by a broad band with absorption centred at 500 cm^{-1}. Inspection of the infrared spectra of mixed and doped oxide hydrate gels show that increasing amounts of iron result in distinct bands in the 300 to 700 cm^{-1} region due to iron–oxygen lattice vibrations, characteristics of α-Fe_2O_3. Incorporation of iron in mixed and doped oxide gels results in a sharpening of the peaks at 790 and 890 cm^{-1}, characteristic of α-FeOOH. These features indicate the formation of zirconium-substituted ferric oxide hydrate gel as the dominant phase, along with some iron-substituted zirconium oxide hydrate gel. The gel structures appear to become more

TABLE I *d*-spacing values calculated from X-ray diffraction patterns of ferric oxide, Fe–Zr mixed oxide and Sn(II)-doped oxide hydrate gels

hkl	*d*-spacings (nm)*		
	Fe oxide	Fe–Zr mixed oxide	Sn(II)-doped oxide
110	0.4185 (100)	0.4180 (100)	0.4182 (100)
130	0.2693 (50)	0.2691 (50)	0.2694 (50)
040	0.2496 (50)	0.2491 (50)	0.2493 (50)
111	0.2454 (25)	0.2458 (25)	0.2457 (25)
140	0.2194 (20)	0.2193 (20)	0.2191 (20)
221	0.1723 (20)	0.1723 (20)	0.1721 (20)
151, 160	0.1564 (18)	0.1561 (18)	0.1567 (18)
061	0.1458 (15)	0.1452 (15)	0.1455 (15)

*The relative intensity values are given in parentheses.

uniform and ordered, as reflected by a sharpening of the bands in the low-frequency region.

3.3. X-ray powder diffraction studies

X-ray diffraction patterns of the ferric oxide hydrate gel show distinct bands from which *d*-spacing values of 0.4185, 0.2693, 0.2496, 0.2194, 0.1723, 0.1564 and 0.1458 nm are observed. These features compare well with the ferric oxide hydrate gel (goethite, α-FeOOH) which is found to belong to the orthorhombic crystal system [14] with $a = 0.4596$, $b = 0.9956$ and $c = 0.3021$ nm. The relative intensity of the diffraction peaks along with the *hkl* values are given in Table I.

X-ray diffraction patterns of Fe–Zr mixed and Sn(II)-doped oxide hydrate gels compare well with the X-ray diffraction pattern of ferric oxide hydrate gel along with some faint, but distinct, reflections indicating the presence of small amounts of Zr(IV) and Sn(II) incorporated therein. *d*-spacing values for these mixed and doped oxide hydrate gels are also mentioned in Table I.

3.4. Transmission electron microscopy

Selected electron micrographs representing the crystal morphology and microstructure of ferric oxide, Fe–Zr mixed oxide and Sn(II)-doped oxide hydrate gels are shown in Fig. 3a to c, respectively.

The electron micrographs of ferric oxide hydrate gel depict it to be composed of large aggregates and small discrete subunit particles with well separated edges. The aggregates which make up the bulk of the gel, have a fibrous morphology.

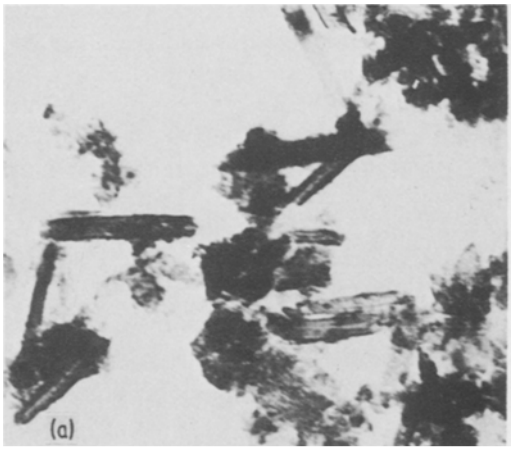

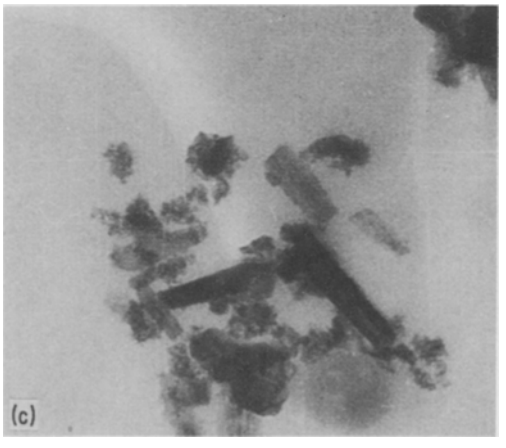

Figure 3 Electron micrographs of hydrate gels: (a) ferric oxide, × 58 000; (b) Fe–Zr mixed oxide, × 58 000; (c) Sn(II)-doped oxide, × 58 000.

The microstructure of the gel is characterized by the presence of two types of phases. The irregular-shaped particles which make-up the bulk of the gel are observed to be aggregates of smaller particles. The long hexagonal to rounded or rectangular plates are probably α-FeOOH or α-Fe_2O_3. The micrographs and the infrared spectra indicate the large hexagonal agglomerates (roughly) to be α-Fe_2O_3. The thin rods (groups of rods) are also agglomerates and are α-FeOOH [15].

Electron micrographs of Fe–Zr mixed and Sn(II)-doped oxide hydrate gels show aggregates similar to those of ferric oxide hydrate gel. The aggregates are composed of hexagonal to rounded and thin rod-like particles joined together resulting in a fine granular and open structure with irregular edges in the bulk aggregates. The incorporation of zirconium and tin into these samples causes a fibrous and fine granular structure in the precipitates, thereby imparting a continuity and coherency to the material.

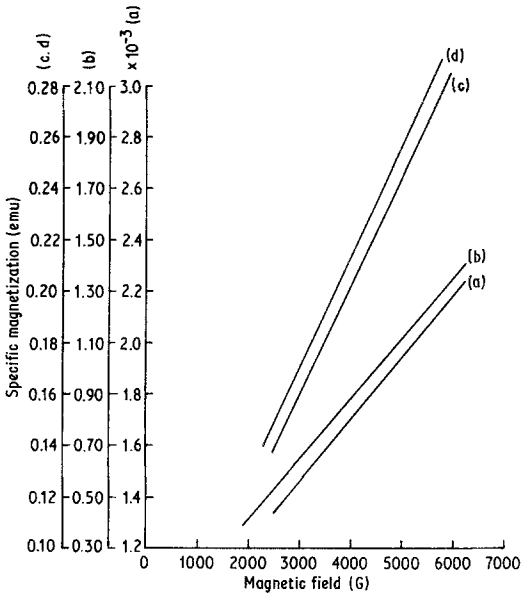

Figure 4 Least-square fitted plots of specific magnetization against magnetic field for hydrate gels: (a) zirconium oxide; (b) ferric oxide; (c) Fe–Zr mixed oxide; (d) Sn(II)-doped oxide.

3.5. Magnetic measurements

Fig. 4 shows the variation of specific magnetization with varying field strength for ferric oxide, zirconium oxide, Fe–Zr mixed and Sn(II)-doped oxide hydrate gels. A summary of the results of magnetic measurements is given in Table II. Room-temperature magnetization of the gels is proportional to the applied field and increases with increasing field value.

The magnetic susceptibility per gram, χ_g, of the ferric oxide hydrate gel is characteristic of incompletely compensated antiferromagnetic particles in the superparamagnetic state. In superparamagnetic antiferromagnets, a decrease in particle size is observed to result in an increase in magnetic susceptibility. This is due to an uncancelled magnetic moment that arises from an imperfect compensation of magnetic moments of the opposite direction in the two magnetic sublattices of the fine particles. Field dependent magnetization and the high value of magnetic susceptibility observed for the gel are in good agreement with the results of various workers [16, 17]. In the case of α-Fe_2O_3, the spins within any (1 1 1) plane are parallel and the adjacent planes are coupled antiferromagnetically. A sharp decrease in χ_g for mixed and doped oxide hydrate gels suggests the formation of an antiferromagnetic mixed phase in the product.

Acknowledgement

One of the authors (CKJ) is grateful to the Council

TABLE II Values of specific magnetization (σ) with varying magnetic field (H) for ferric oxide, zirconium oxide, Fe–Zr mixed oxide and Sn(II)-doped oxide hydrate gels

Field (G)	Specific magnetization (emu)			
	Fe oxide	Zr oxide	Fe–Zr mixed oxide	Sn(II)-doped oxide
2500	0.532	1.340×10^{-3}	0.137	0.146
3700	0.791	1.650×10^{-3}	0.188	0.199
4800	1.060	1.880×10^{-3}	0.233	0.243
5800	1.301	2.180×10^{-3}	0.276	0.289
χ_g ($\times 10^{-6}$)	233.3	0.241	40.0	42.0

Values of χ_g have been calculated from the linear plots of specific magnetization against field strength.

of Scientific and Industrial Research, New Delhi, India, for financing this research project.

References

1. D. J. CRAIK (ed), "Magnetic Oxides" (Wiley, London, New York, 1975) pp. 649–686, 687–742, 743–776.
2. C. N. R. RAO, in "Transition Metal Oxides in Solid State Chemistry" (Marcel Dekker, New York, 1974) p. 455.
3. N. C. DUTTA, *J. Sci. Ind. Res.* **40** (1981) 571.
4. M. E. WINFIELD, in "Catalysis", Vol. 7, edited by P. H. Emmett (Reinhold, New York, 1960) p. 93.
5. J. R. ANDERSON, in "Structure of Mettalic Catalysts" (Academic Press, New York, 1975) p. 63.
6. M. J. TORRALVO-FERNANDEZ and M. A. ALARIO-FRANCO, *J. Colloid Interface Sci.* 77 (1980) 29.
7. R. M. VEST, M. M. THALLAN and W. C. TRIPP, *J. Amer. Ceram. Soc.* **47** (1964) 635.
8. F. G. R. GIMBLET, A. A. RAHMAN and K. S. W. SINGH, *J. Chem. Tech. Biotech.* **30** (1980) 51.
9. W. SMYKATZ-KLOSS, in "Differential Thermal Analysis" (Springer Verlag, Berlin, Heidelberg, New York, 1974) p. 37.
10. R. C. MACKENZIE and G. BERGGREN, in "Differential Thermal Analysis", Vol. 1, edited by R. C. Mackenzie (Academic Press, London, 1970) p. 272.
11. Y. I. RYSKIN, in "The Infrared Spectra of Minerals", edited by V. C. Farmer (Mineralogical Society, London, 1974) p. 137.
12. R. A. NYQUIST and R. O. KAGEL, in "Infrared Spectra of Inorganic Compounds" (Academic Press, New York, 1971).
13. K. KAUFFMAN and F. HAZEL, *J. Inorg. Nucl. Chem.* **37** (1975) 1139.
14. C. G. A. HARRISON and M. N. A. PETERSON, *Amer. Mineral.* **50** (1965) 704.
15. W. FEITKNECHT and W. MICHAELIS, *Helv. Chim. Acta* **45** (1962) 212.
16. A. A. VAN DER GIESSEN, *Phillips Res. Rep. Suppl.* **12** (1968) 104.
17. G. MATZEN and P. POIX, *J. Mater. Sci.* **17** (1982) 701.

Received 2 April
and accepted 16 May 1984